ELSEVIER

Ceramics International 30 (2004) 1–7

CERAMICS INTERNATIONAL

www.elsevier.com/locate/ceramint

The state of iron impurities in a beryllium ceramic as determined from NGRS data

V.A. Shabashov[a], V.S. Kijko[b,*], I.A. Dmitriev[b], A.G. Mukoseev[a]

[a]*Institute of Metal Physics, Ural Branch RAS, S.Kovalevskaya st. 18, 620219 Ekaterinburg, Russian Federation*
[b]*Ural State Technical University, Ê-2, Mira st.28, 620002 Ekaterinburg, Russian Federation*

Received 12 December 2002; received in revised form 20 December 2002; accepted 20 February 2003

Abstract

Iron impurities influence the sintering process of the BeO ceramic, its physical–chemical and performance characteristics. These impurities may concentrate in different areas of products during sintering and cause their coloring. The state of iron impurities in white-, gray-, and dark-color samples of a commercial BeO ceramic was studied by the methods of Mössbauer spectroscopy, electron paramagnetic resonance, and X-ray analysis. It was found that the total concentration of the iron impurity was smaller in the white samples than in the gray and blacks samples of the BeO ceramic. The white samples contained iron mostly in the form of α-Fe_2O_3 oxides or metallic iron. A higher intensity of the ceramic coloring corresponded to an increase in the iron concentration of beryllium solid solutions and their carbide and intermetallic derivatives.

Keywords: A. Sintering; B. Spectroscopy; C. Colour; D. BeO; E. Substrates

1. Introduction

The beryllium-oxide-based ceramic has some unique properties and is used in metallurgy, laser equipment, ionizing radiation dosimetry, and modern electronics. The study of the state of iron impurities in the BeO ceramic is very significant since it is used on a progressively wider scale in computers, radio and TV equipment, military technologies, spacecraft, and other highly dependable applications.

A chemical analysis of a commercial sintered BeO ceramic showed that it contained Fe, Si, Al, Ca and C impurities implanted from the initial BeO powder and during the ceramic synthesis. The concentration of iron impurities, which was between $8{\cdot}10^{-3}$ and $1{\cdot}10^{-1}$ mass%, was the largest. It was found that even a small quantity of iron impurities had a decisive effect on physical-chemical and operating properties of the ceramic.

A number of studies, for example [1–7], have been dedicated to the effect of iron impurities on physical-chemical properties and sintering of the beryllium ceramic. The iron impurity shows the greatest promise since a small addition of the iron impurity provides a high density (0.01–0.3 mass%) of this ceramic. In accordance with [4,5], if the iron concentration exceeds 0.4 mass%, the sintering ability of the ceramic decreases because of the formation of a new phase.

When the BeO ceramic is sintered in a graphite charge in high-temperature furnaces outfitted with graphite heaters, the higher iron oxide, which is present in the initial BeO powder, is reduced as follows: α-Fe_2O_3 → γ-Fe_2O_3 → Fe_3O_4 → FeO → Fe. This scheme of reduction and an obstructed diffusion of the reducing gas (CO) to the bulk of the sintered ceramic cause a spatial differentiation of the reduction phases of the iron oxides, leading to formation of Fe_2O_3/Fe_3O_4, Fe_3O_4/FeO and FeO/Fe interfaces, which follow one another to the center of the ceramic, and appearance of zonal dyeing. In Refs. [6,7] have been analyzed the causes responsible for an inhomogeneous structure and zonal dyeing (white, gray and dark colors) of commercial products made of the BeO ceramic, which did not contain deliberate additions of iron impurities. It was found that different-size grains of the microstructure in the cross-section of the products, which affected their performance, were caused by iron impurities. Microcrystals of

* Corresponding author. Tel.: +7-3432-754432.
E-mail address: kijko@fsm.ustu.ru (V.S. Kijko).

0272-8842/03/$30.00
doi:10.1016/S0272-8842(03)00054-3

BeO in colored zones were 1.5–3.5 times larger on the average than those in the white zone.

An examination by the methods of electron paramagnetic resonance (EPR) and optical absorption showed [6] that zonal dyeing and coarsening of grains in the ceramic products were due to inclusions of Fe^{3+} ions in the crystal lattice of BeO and appearance of surface formations on BeO single crystals. The process of phase formation in a beryllium ceramic was studied [7] by the method of magnetic susceptibility χ. The field dependence $\chi(H)$ was observed at room temperature in samples, which were cut from the white and gray zones of one and the same product. This dependence suggested the presence of ferromagnetic impurities probably in the form of γ-Fe_2O_3 and Fe_3O_4 or their solid solutions. The quantity of the ferromagnetic phase was much smaller in white-color samples than in gray-color samples. An analysis of the temperature dependence of χ, which was measured in a vacuum and an inert gas atmosphere, showed that the white-color samples of the ceramic contained, in addition to ferromagnetic oxides (γ-Fe_2O_3 and Fe_3O_4), some quantity of reduced metallic iron, which was oxidized when the ceramic was heated in a forevacuum ($\sim$1 Pa) at a temperature of 900 °C. The quantity of metallic iron was much smaller in the gray-color ceramic than in the white-color ceramic. The ferromagnetic oxides transformed, but not completely, to antiferromagnetic α-Fe_2O_3 when the ceramic was heated in a vacuum or helium at 1170 K. The samples had to be held for a long time at this temperature to accomplish a complete transformation to α-Fe_2O_3.

The EPR data were suggestive that the gray and dark-gray samples included a superparamagnetic phase with a strong Fe^{3+}–Fe^{3+} exchange interaction probably of clusters type Fe^{3+}–O^2–Fe^{3+} and Fe^{3+}–O^2–Fe^{2+} having different dimensions [6,7].

The χ values for the samples with an intense dark-gray color were three or more times larger than χ for the gray sample and one order of magnitude larger than those for the white-color sample. One might assume that the dark-gray samples of the ceramic contained iron bound to some compound (surrounded by ions of another element) and/or compounds whose structure could not be determined [7].

The Mössbauer spectroscopy method was used to determine most fully the phase composition of iron impurities in the BeO ceramic, which was colored differently after sintering. In addition, the methods of X-ray diffraction analysis and EPR were used in this study.

2. Samples and measurement technique

Samples from different lots of a commercial BeO ceramic including iron impurities (entrapped in the ceramic from the initial BeO powder or during technological stages of the ceramic production) were analyzed. The samples were colored differently (white, gray and black). They were prepared using a standard ceramic technology (batch A: semi-dry compaction or slip-cast molding; batch B: a film technology). The samples were sintered in a high-temperature vacuum box furnace with graphite heaters at a temperature from 1830 to 1920 C.

The samples were tested for transparency to the Mössbauer radiation (14.4 keV) from a$\sim$100 mKu ^{57}Co (Cr) source. The absorbing samples were stacked up so that the ratio between the transmitted Mössbauer radiation and the background was the same. Therefore, it was possible to estimate the quantity of iron in the samples from the ratio of integral intensities of the spectra. The measurements were made using the same geometry with a 25-mm collimator. The concentration of the ^{57}Fe resonance isotope in the impurity iron corresponded to the natural concentration of $\sim$2–3%.

The measurements were made in three ranges of the velocity scale: $-10\ldots+10$ mm/s, $-5\ldots+5$ mm/s, and $-3\ldots+3$ mm/s. The third range was necessary for a more detailed analysis of the structure of the main part of nonmagnetic components in the Mössbauer spectra.

Since the concentration of the ^{57}Fe isotope was small, a "DISTRI" software package, which improved the spectra resolution (reconstruction of the density functions of the Mössbauer parameters) by means of a regularization procedure, was used. The density function of the centers of gravity of absorption resonance lines P(V) was reconstructed. An elementary absorption line was a Lorentzian with internal lines of the Zeeman sextet of the reference iron being $\sim$0.20 mm/s wide.

The P(V) function was approximated by a linear combination of modified Gaussian lines to determine individual distributions corresponding to different atomic configurations of iron in the structure of the test samples.

The P(V) data were used for modeling and direct calculation of subspectra with the corresponding Mössbauer parameters by the method of the least misfit (the "SPECTR" program) between the theoretical and experimental spectra.

Paramagnetic impurities in the samples were determined at room temperature using the EPR method. Signals corresponding to Fe^{3+} ions in different states were recorded.

An X-ray diffraction analysis of dyed samples of the BeO ceramic was performed on a "DRON-2" diffractometer. The X-ray installation was adjusted to a maximum sensitivity, which ensured recording of small quantities of impurity phases as compared to the quantity of BeO.

3. Experimental results

According to the EPR data, the spectroscopic parameters of the black samples from the batch B, which were not exposed to ionizing radiation, were $g = 2.73$ and $\Delta H = 2030$ G, while those of the gray samples from the batches A and B were $g = 2.28$ and $\Delta H = 1210$ G, and $g = 2.26$ and $\Delta H = 1400$ G, respectively. It was found that the signals were due to Fe^{3+} ions in different structural states. EPR signals were not detected in the gray samples from the batches A and B.

Since the X-ray diffraction analysis provided a weak sensitivity, a new phase corresponding to a small quantity (2–3 mass%) of the Fe_3C iron carbide was detected only in the black samples of the BeO ceramic.

The structure of the Mössbauer spectra of the BeO ceramic samples was determined. The measurements at a velocity from −10 to +10 mm/s showed that the central part in the form of a peak with a complicated structure was prominent in the spectra of the white, gray and black samples against a set of Zeeman splittings with a wide range of the fields (from the oxide range to the iron one and smaller). The set of Zeeman splittings in the spectra was poorly resolved, but generally had an analogous structure. The spectra exhibited sextets with fields of iron oxides and metallic iron, and sextets with intermediate fields, which were due probably to a relaxation in the oxide structure. The measurements at a velocity from −10 to +10 mm/s showed that the total surface area of the spectra recorded for the gray samples was much larger (more than 2 times) than the total surface area of the spectra obtained for the white samples (Fig. 1 and Table 1). A higher integral intensity of the spectra from the gray and black samples and an improvement of the signal-to-noise ratio could be explained by an increase in the total quantity of the resonance iron in the samples. An increase in the integral intensity of the absorption spectra could be due partly to a higher probability of the Mössbauer effect [8,9]. The integral intensities of the Zeeman part of the spectra from the white and gray samples differed little. This part of the structure had the lowest intensity in the black sample (see Table 1). The spectra differed mainly in the ratios of the components present in their central part. The integral intensity of the central part of the spectra from the gray and black samples was at least 5 times larger than that obtained from the white samples.

The high-resolution (the interval of −3 to +3 mm/s) measurements in the central part of the spectrum showed that this part of the spectrum from the white samples comprised an asymmetric "doublet". This "doublet" could be caused partly by relaxation processes and the summation of contributions from internal lines of superimposed sextets. However, random (uncontrolled) variations of the ratio between the left- and right-hand lines of the "doublet" depending on the batch of the samples [see spectra *a*, *b* and density functions P(V) *a*′, *b*′, Fig. 2] allowed assuming a contribution to these lines from separate phases determined from the Mössbauer parameters. The left-hand line had an isomer shift (IS) approaching IS of metallic iron and its intermetallic compounds, i.e. iron was in a low-spin state characteristic of metallic compounds of iron having good conductivity. The isomer shift of the right-hand line referred it to iron oxides (α- and γ-Fe_2O_3, and tetrahedral sites in inverse $Fe_{3-\nu}O_4$ spinel).

The spectra from the gray samples preserved the structure of the spectra from the white samples, but they exhibited changes in their central part (see *c*–*c*′ and *d*–*d*′

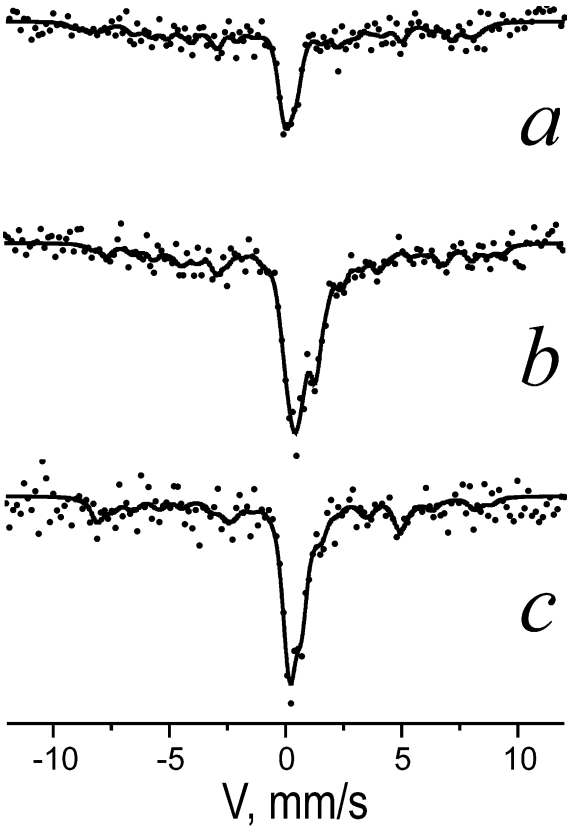

Fig. 1. Gamma resonance spectra of differently colored samples of the beryllium oxide ceramic (*a*—white, *b*—gray, *c*—black) in a large interval of velocities (−10…+10 mm/s).

Table 1
Integral intensities[a] of components in the Zeeman and central parts of the spectra

Part of spectrum	White sample		Gray sample		Black sample
	Batch A	Batch B	Batch A	Batch B	Batch B
Zeeman	2/–	2/–	3/1	2/1	1/0.5
Central	1	0.8	6	8	4

[a] The unity is assumed to be the surface area of the central component in the white sample from batch A; the intensities of the general/carbide components were distinguished for the Zeeman component.

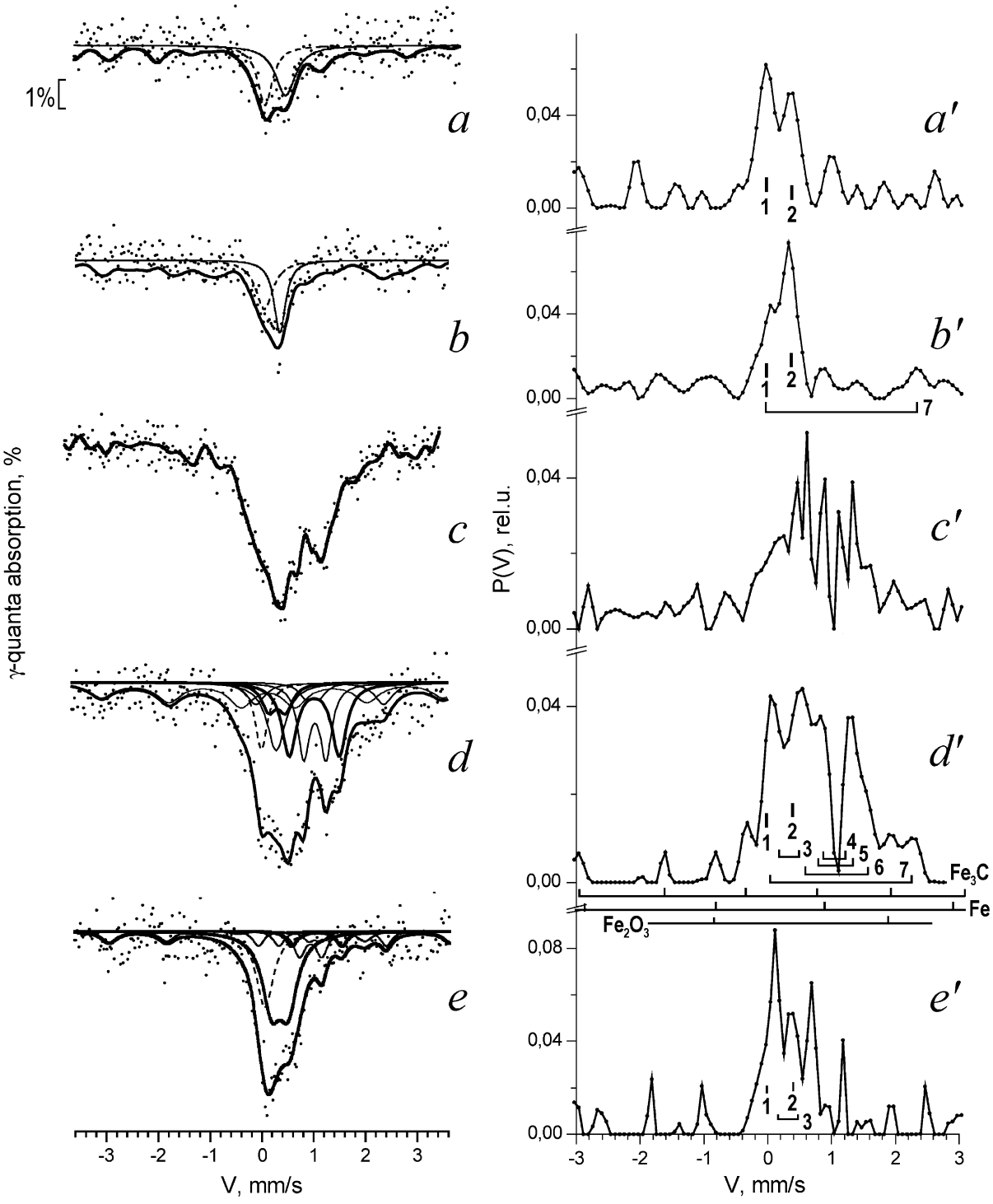

Fig. 2. Gamma resonance spectra (*a*–*e*) and distribution functions P(V) (*a*′–*e*′) of differently colored (white, gray, and black) samples of the beryllium oxide ceramic in a small interval of velocities from −3 to +3 mm/s: *a*–*a*′, *b*–*b*′—white samples from batches A and B respectively; *c*–*c*′, *d*–*d*′—gray samples from batches A and B respectively; *e*–*e*′—black sample from batch B.

in Fig. 2). As the first approximation, the spectra were described by an additional doublet 3 with IS equal to 0.34 mm/s, a quadrupole splitting (QS) equal to 0.28 mm/s, and other doublets with isomer shifts of the wustite range (0.8–1.0 mm/s relative to α-Fe) and largely different QS. A doublet 7 with IS = 1.17 mm/s and QS = 2.46 mm/s was prominent in the superposition of the doublets shifted to the region of positive velocities. Notice that similarly to the white samples, the spectra from different gray samples of the batches A and B had some specific features, which distinguished them from the spectra of samples having a different color intensity.

In the case of the gray samples, these specific features included a large integral intensity of the doublets 4, 5 and 6. An additional group of doublets with velocities shifted for 0.8–1 mm/s was represented on a much smaller scale in the spectrum from the black sample (*e*–*e*′ in Fig. 2). A specific feature of the black sample was a predominant partial contribution from the doublet 3 and the first (metallic) component of the spectrum, while the oxide Zeeman part was nearly absent. Sextets with fields approaching β-$FeBe_{2+x}$ and Fe_3C were pronounced well too. Considerable quantities of α-Fe and the Fe_2O_3 oxide were detected in all the spectra from the white, gray and black samples.

4. Discussion

From the spectral analysis described above it follows that the spectra of the white, gray and black samples, on the one hand, are complex and different, and, on the other hand, have a similar structure. In all the cases, three groups of components of the iron-containing structure can be distinguished in the spectra obtained for the BeO ceramic. These groups include (1) components corresponding to a low-spin "metallic" state of iron (IS = −0.1 to 0.4 mm/s), (2) oxide compounds with IS from 0.4 to 0.5 mm/s, and (3) oxides of the wustite range with IS > 0.8 mm/s. The first two groups comprise both sextets and lines without the Zeeman splitting. The third group is presented as a superposition of quadrupole-splitting doublets.

The spectral components were calculated and interpreted assuming a common structure of the spectra, additivity of separate components, and the possibility that they make different contributions to the total integral spectrum. An a priori Mössbauer information about possible phases and the structure in the system under study was used.

Therefore, the spectra from the white samples, namely, the first line (see 1 in *a*′, Fig. 2) may comprise a paramagnetic structure of the carbon austenite, superparamagnetic iron, and ε-$FeBe_5$ beryllides [10–12]. The left-hand line corresponds to γ-Fe by IS [13]. It should be noted that the spectra of the iron-containing structure included predominantly spectra of α- and γ-Fe in some ceramic sintering experiments. The presence of γ-Fe may be related to a high diffusion mobility of beryllium and the carbon impurity, which diffuse to iron at a high annealing temperature and stabilize paramagnetic γ-Fe solid solutions. The fact that the α-Fe spectra contain components of solid solutions having smaller effective fields points to the possible formation of the whole set of compositions comprising the Fe–Be system [10, 12]. The right-hand line, which corresponds by IS to the interval of iron-containing oxides with the Fe^{3+} valence [10–12], may result from relaxation phenomena, amorphization, and the state of the interface of the α-Fe_2O_3–γ-Fe_2O_3 type in the structure [14–17] when some iron cations are replaced by beryllium. The left- and right-hand lines may be superimposed by lines of doublets of Be(Fe) solid solutions and the higher $FeBe_{12}$ beryllide [10]. Most iron in the white samples (see *a*–*a*′ in Fig. 2) is represented by Zeeman sextets of the α-Fe(Be) ferromagnetic structure and, probably, iron oxides, such as α-Fe_2O_3, $Fe_{3-y}O_4$, and γ-Fe_2O_3 [18–21]. The doublets 4, 5 and 6 are nearly absent and the doublet 7 is present in the structure of the white samples. A similar structure (the doublet 7) was observed [22] when γ-Fe clusters were oxidized in a heavily diluted Cu–0.2 at.% Fe alloy. As in [22], the doublet 7 may probably be referred to the initial stage of internal oxidation of near-surface iron clusters.

As was noted in the foregoing, many more iron atoms are present in the structure of the gray samples, which is described by the central part of the spectrum. As regards the central part of the spectrum namely the doublet 3, one may state that this doublet may be due to $Be_mFe_nC_p$ compounds [10] and, probably, iron oxycarbides with a variable composition $Fe_xO_yC_z$. Notice also that a doublet having similar parameters was observed in iron carbides, which were extracted from steels and annealed [18]. In addition to this structure, doublets analogous to wustite doublets [19] (see the doublets 4, 5, 6, 7 in *c*–*c*′ and *d*–*d*′, Fig. 2) are prominent. A more complicated structure of the spectra may be explained by iron impurities in beryllium and its oxides, i.e. Be(Fe)O. Moreover, lines of the β-$FeBe_{2+x}$ and Fe_3C sextets stand out [12,18]. Thus, it is seen that carbon- and beryllium-containing iron compounds are formed and iron-bearing structures with a higher concentration of Be appear in the gray samples. It was shown in the foregoing that despite a general analogy, the spectrum from the black sample contains a small number of sextets of the oxide range (see *e*–*e*′ in Fig. 2) as distinct from the spectrum of the white samples, and a small fraction of the structure of the wustite range as distinct from the spectrum of the gray samples. However, the intensity of the lines corresponding to carbide- and beryllium-containing iron compounds $Be_mFe_nC_p$, and Be(Fe)O, ε-$BeFe_5$, $FeBe_x$ and γ-FeC is enhanced considerably in the structure of the black sample. In addition, sextets of β-$FeBe_{2+x}$ and the Fe_3C carbide are more intense than in the white samples.

Variations of the partial contribution from superposition spectra are specified in Table 2 in order to trace the possible relation between the structure of the central part of the spectra and the intensity of the black color. From Tables 1–4 it follows unambiguously that the total quantity of iron in the structure of the beryllium ceramic is not the only factor determining the intensity of the black color. This conclusion is evident from a comparison of the spectra obtained for the gray and black samples.

Table 2
Mössbauer parameters of non-Zeeman components in the central part of the spectra (A/B) from the white samples

Spectral components	1	2	3	4	5	6	7
IS (±0.005), mm/s	0.036/−0.034	0.360/0.400	–/0.345	–	–	–	–/1.170
QS (±0.01), mm/s	–	–	–/0.32	–	–	–	–/2.46
Partial contribution A/B, (±10)%	55/20	40/50	–/10	–	–	–	–/20

Table 3
Mössbauer parameters of non-Zeeman components in the central part of the spectra (A/B) from the gray samples in batch B

Spectral components	1	2	3	4	5	6	7
IS (±0.005), mm/s	−0.040	0.327	0.345	1.024	1.073	1.060	1.167
QS (±0.01), mm/s	–	–	0.32	0.25	0.43	0.96	2.46
Partial contribution A/B, (±)%	10	15	10	6	21	27	10

Table 4
Mössbauer parameters of non-Zeeman components in the central part of the spectrum from the black sample

Spectral components	1	2	3	4	5	6	7
IS (±0.005), mm/s	0.056	0.327	0.345	1.024	0.940	1.060	1.167
QS (±0.01), mm/s	–	–	0.32	0.25	0.43	0.96	2.46
Partial contribution, (±5)%	24	4	46	3	10	6	6

A higher integral intensity of the gray samples is distributed in Zeeman (oxide and α-Fe) parts of the structure and the Be(Fe)O structure. The spectra of the black samples are dominated by central groups of lines 1 and 2 and especially the doublet 3, which are due to appearance of $Be_mFe_nC_p$ structures, higher $FeBe_x$ beryllides, and Be(Fe)O and γ-FeC solid solutions. The Zeeman part of the structure of the black sample also contains mostly iron compounds with beryllium and carbon, β-$FeBe_{2+x}$ and Fe_3C. It is these components that dominate in the spectrum of the black sample with respect to both their relative and absolute values. The appearance of this structure obviously depends on the total quantity of iron in the ceramic sample, but, probably, is determined mainly by thermodynamic conditions of the ceramic sintering process. As a result, iron does not substitute beryllium in the oxide, but forms metallic solid solutions and compounds with beryllium and carbon. In particular, considering the data reported in Ref. [12], one may expect that iron carbides and beryllides are formed during sintering if free iron and carbon are present in the initial material. This situation is actually observed in the gray and black samples. A high sintering temperature is conducive to decomposition of carbides and beryllides, which is followed by formation of α-FeBe and FeC solid solutions. Iron passes to the beryllium oxide simultaneously. These processes are typical of the white samples. Subsequent darkening of the samples may probably be related to formation of iron beryllides and carbides from solid solutions.

5. Conclusion

The total concentration of the iron impurity was smaller in the white samples than in the gray and black samples of the beryllium ceramic. The iron impurity was present in these samples as oxides or metal iron. All the samples contained some quantity of elemental (free) iron. The appearance of the spectra, namely, the ratio of resolved components and their total number correlate with coloring of the samples.

A heavier coloring of the ceramic samples corresponded to an increase in the beryllium concentration of the iron solid solutions and their carbide and intermetallic derivatives. The gray and black samples contained a ferromagnetic structure (in a sufficiently large quantity). The quantity of the carbide phase in the gray samples was smaller than in the black sample thanks to formation of a large volume of a Be(Fe)O-type structure. An increase in ''magnetization'' of the black and, especially, gray samples could be explained not only by the presence of iron carbides and oxycarbides, but also by a high concentration of ferromagnetic and superparamagnetic iron.

Variation of the intensity of the black color in the ceramic samples correlated with an increase in the volume of nonmagnetic structures of the Be(Fe)O type and a high concentration of Fe_3C.

From the Mössbauer spectra it followed that iron impurities in the BeO ceramic could be represented by:

1. Ions substituting some Be^{2+} ions in the cation sublattice of BeO;
2. Be–Fe intermetallic compounds;
3. Surface formations like Be–Fe–O, FeC, and $Be_mFe_nC_p$ or iron oxycarbides $Fe_xO_yC_z$;
4. Ferromagnetic and superparamagnetic structures forming a separate phase and located on the surface and boundaries of microcrystals and pores.

References

[1] R.A. Belyaev, Beryllium Oxide, Atomizdat, Moscow, 1980.

[2] E.G. Semin, Yu.N. Lukin, N.A. Andreeva, Dynamics of compaction and growth of beryllium oxide grains in the presence of iron oxide, Neorgan, Materialy 22 (1986) 623–626.

[3] Bhat R. Moorthy, Sintering of beryllium oxide—influence of minor additions on densification and microstructural development, Trans. Ind. Ceram. Soc. 32 (1973) 1–10.

[4] E.G. Semin, L.V. Zubenko, G.V. Cerepkov, Physical-chemical study of BeO–Fe_2O_3-based catalysts of dehydrogenation and dehydrocycling, in: Study of Heterogeneous Catalytic Processes, Leningrad Tech. Institute Publ., Leningrad, 1976, pp. 80–86.

[5] E.G. Semin, Physical-chemical study of the BeO–Fe_2O_3 system, Zhurn. Phis. Khimii 49 (1975) 2451–2456.

[6] V.S. Kijko, I.A. Dmitriev, I.D. Kascheev, Cause of dyeing of beryllium ceramic, Neorgan, Materialy 27 (1991) 1945–1947.

[7] V.S. Kijko, I.I. Piratinskaya, Yu.A. Vereschagin, Effect of iron impurities on coloring of beryllium ceramic, Neorgan, Materialy 28 (1992) 1786–1791.

[8] Ya.A. Fedorovsky, T.S. Gendler, K.P. Mitrovanov, M.V. Plotnikova, Glass, Proceedings of Institute of Glass 1 (1966) 93–98.

[9] R.N. Kuzmin, T.S. Gendler, Study of structural-magnetic phase transformations in siderite, Kristallografiya 15 (1970) 736–741.

[10] L.A. Alekseev, Yu.F. Babikova, V.P. Gladkov, V.S. Zotov, V.I. Kondar, D.M. Skorov, Study of alloys of the Fe–Be–C system by the method of nuclear gamma resonance, Atomnaya Energiya 35 (1973) 173–174.

[11] S.N. Belozersky, V.N., Gittsovich, S.V. Lubarsky, L.V. Kurashkin, Yu.P. Khimich, An application of Mössbauer spectroscopy on ^{57}Fe for investigation of Be, Proc. XX Congress AMPERE, Tallin, 1978, D-4301, Berlin, 1979, p. 249.

[12] K.K. Kadyrzhanov, V.S. Rusakov, T.E. Turkebaev, E.A. Karimov, M.F. Vereshchak, A.D. Lopuga, Mössbauer studies of thermal effect: impact of beryllium-coated iron, Bulletin of the Russian Academy of Science, Physics 7 (2001) 1107–1112.

[13] V.A. Shabashov, L.G. Korshunov, A.G. Mukoseev, Deformation-induced phase transformation in a high-carbon steel, Mater. Sci. Eng. A 346 (1–2) (2003) 196–207.

[14] S. Morup, H. Torsoe, Y. Lipka, Modified theory for Mössbauer spectra of superparamagnetic particles: application to Fe_3O_4, J. de Physique 37 (1976) 287–290.

[15] B. Kopcewich, M. Kopcewich, Investigation of iron containing atmospheric aerosols, J. de Physique 37 (1976) 841–844.

[16] P. Ayyt, M. Maltani, M. Barma, V.R. Palkar, R. Vijayarajanan, Size-induced structural phase transitions and hyperfine properties of microcrystalline Fe_2O_3, J. Phys. S. Solid. 2 (1988) 2229–2245, (printed in the UK).

[17] I.P. Suzdalev, V.N. Buravtsev, V.K. Imshennik, M.V. Maksimov, V.V. Matveev, Magnetic and structural phase transitions in iron oxide nanosystems: impact of interfaces, Bulletin of the Russian Academy of Science, Physics 7 (2001) 1113–1117.

[18] Z. Mathalone, M. Ron, J. Pipman, S. Niedgwieds, Mössbauer characteristics of ϵ, χ and θ carbides, J. Appl. Phys. 42 (1971) 687–695.

[19] F. Van der Woude, Mössbauer effect in α Fe_2O_3, Phys. Stat. Sol. 17 (1966) 417–432.

[20] J.M. Daniels, A. Rosencwaig, Mössbauer spectroscopy of stoichiometric and non-stoichiometric magnetite, J. Phys. Chem. Solids 30 (1969) 1561–1571.

[21] H. Annersten, S.S. Hetner, Vacancy distribution in synthetic spinels of series Fe_3O_4–γ Fe_2O_3, Zeitschrify für Kristallographie 137 (1973) 321–340.

[22] D.L. Williamson, M. Ellid, Temperature study of a Cu–0.2 at. % Fe alloy, J. de Physique 40 (1979) 601–603.